

Numerical Study of the One-Dimensional Spin-Orbit Coupled System with $SU(2) \otimes SU(2)$ Symmetry

Yasufumi Yamashita, Naokazu Shibata¹, and Kazuo Ueda

Institute for Solid State Physics, University of Tokyo, Roppongi 7-22-1, Minatoku, Tokyo 106-8666, Japan

¹*Institute of Material Physics, University of Tsukuba, Tsukuba 305-8573, Japan.*

(Received September 26, 2018)

We numerically study the $SU(2) \otimes SU(2)$ symmetric spin-orbit coupled model as a lower symmetric generalization of the $SU(4)$ exchange model. On the symmetric line with respect to the spin and orbit, our result shows the essentially singular gap formation in consistent with the analytic approach, which is different from the previous numerical calculation. Furthermore, we find new critical phases around the $SU(4)$ point, surrounding the previously known gapless symmetric line. In these novel phases either spin or orbital excitations around momentum $q = \pi$ form massless continua which split from the excitations belonging to the $[2^2]$ irreducible representation at the $SU(4)$ point. On the critical symmetric line, the additional coupled spin-orbit excitations around $q = \pi/2$ originating from $[2^1 1^2]$ become critical, too.

KEYWORDS: spin-orbit coupled system, orbital fluctuations, $SU(4)$ symmetry, DMRG

§1. Introduction

In connection with the study of the spin-orbit coupled systems with strong quantum fluctuations, the highest symmetric $SU(4)$ exchange model has been a subject of the intensive study.^{1,2,3)} It describes the localized model of the orbitally twofold degenerate Hubbard model with the hoppings between the same type of the orbitals, neglecting Hund rule coupling. The fundamental understandings of this most simplified model have been obtained beyond the scope of the mean-field analysis in one dimension. In realistic materials, however, the highest $SU(4)$ symmetry is almost always broken by an anisotropic hybridization or Jahn-Teller effect. Therefore, it is interesting as a next step to consider the physically relevant lower symmetric models around the $SU(4)$ symmetric limit, which may shed light on the physics of recent interest concerned with the spin and orbital fluctuations. For example, we studied the $SU(4)$ exchange model under magnetic fields with the resultant $SU(2) \otimes U(1)$ symmetry and found the crossover phenomena between the $SU(4)$ and the $S(2)$ symmetric limit.⁴⁾ As another example, a finite Hund coupling constant introduce the Ising-type anisotropy into the orbital part of the effective Hamiltonian, while the spin part keeps the $SU(2)$ symmetry.¹⁾

As a different lower symmetric model, the following $SU(2) \otimes SU(2)$ symmetric model has been studied by using the numerical and/or analytical method by several authors;^{5,6)}

$$H(a, b) = K \sum_i \left(\vec{S}_i \vec{S}_{i+1} + \frac{a}{4} \right) \left(\vec{T}_i \vec{T}_{i+1} + \frac{b}{4} \right), \quad (1)$$

where K is a positive constant and \vec{S} and \vec{T} are the spin and orbital pseudo-spin $1/2$ operators, respectively.

The study of this seemingly artificial model is stimulated by the recent experimental progresses in the quasi one-dimensional spin-gap materials such as $Na_2Ti_2Sb_2O$ or NaV_2O_5 , which are essentially described by the two-band Hubbard model at quarter filling.⁵⁾ Kolezhuk *et al.*⁷⁾ studied $H(3,3)$ by using the matrix product ansatz and showed that this model has the doubly degenerate ground states with gapful excitations. Note that, in our definition, $H(1,1)$ is equal to the integrable $SU(4)$ exchange model and gapless.^{1,2)} Pati *et al.*⁵⁾ studied the model by using the density matrix renormalization group (DMRG) method, but their results are significantly different from ours in the most interesting region in the $a-b$ plane. On the symmetric $b = a$ line, our results are consistent with those of the recent analysis applying the bosonization method around the $SU(4)$ symmetric point by Azaria *et al.*⁶⁾

The purpose of this paper is to present a renewed phase diagram over the entire $a-b$ plane, including newly found critical phases sandwiching the previously known gapless symmetric line. The four distinct phases centering the $SU(4)$ symmetric point are classified with the aid of the Lieb-Schultz-Mattis (LSM) theorem. We are benefited from the Bethe-ansatz results of the three massless $SU(4)$ -multiplet excitations and how they split away from the $SU(4)$ point. The concept of the simple renormalization group around the $SU(4)$ fixed point has also helps us to draw the gapless-gapful phase boundaries.

§2. Ground-state properties and Magnetic phase diagram

Let us begin our analysis by investigating the ground-state properties of $H(a, b)$ by using the Lanczos and DMRG method.⁸⁾ Though Pati *et al.* have performed similar calculations, their results are over-simplified. So

we present more detailed ground-state phase diagram including asymptotic behaviors and some exact proofs about these phases. In what follows, we mainly use the periodic boundary conditions (PBC) for eliminating the boundary effects and consider the $N = 4n$ number of sites to avoid the extrinsic effects due to the complex many-fold degeneracies.¹⁾ The ground-states phase diagram in the two-dimensional $a - b$ plane is illustrated in Fig.1. By the numerical calculations with changing the system sizes up to 20 sites, we have confirmed that the phase boundaries hardly move.

Besides the SU(4) symmetric point at $(a, b) = (1, 1)$, where the model is Bethe-ansatz integrable, we can show that there are several regions in the $a - b$ plane where the ground states are determined exactly. In the region III ($a \leq -1$ and $b \leq -1$), we can prove the following inequality;

$$\begin{aligned} H(a, b) &= \sum_i \left(\frac{1}{4} - \vec{S}_i \vec{S}_{i+1} + |a_+| \right) \left(\frac{1}{4} - \vec{T}_i \vec{T}_{i+1} + |b_+| \right) \\ &= \sum_i (P_{i,i+1}^{S=0} P_{i,i+1}^{T=0} + |b_+| P_{i,i+1}^{S=0} + |a_+| P_{i,i+1}^{T=0} + a_+ b_+) \\ &\geq \sum_i (a+1)(b+1)/16, \end{aligned} \quad (2)$$

where $a_+ = (a+1)/4$ and $b_+ = (b+1)/4$, and $P_{i,i+1}^{S=0}$ ($P_{i,i+1}^{T=0}$) is the projection operator onto the S (T) spin singlet for the neighboring sites. The equality is satisfied when and only when both S and T spins order ferromagnetically. Accordingly, the ground state is the complete ferromagnetic state with respect to both S and T spins.

In the part of phase IV ($a \geq -1$ and $b \leq -1$), we can rewrite the $H(a, b)$ as follows;

$$\begin{aligned} H(a, b) &= \sum_i \left(\frac{1}{4} - \vec{S}_i \vec{S}_{i+1} - a_+ \right) \left(\frac{1}{4} - \vec{T}_i \vec{T}_{i+1} + |b_+| \right) \\ &= \sum_i (P_{i,i+1}^{S=0} P_{i,i+1}^{T=0} + |b_+| P_{i,i+1}^{S=0} - a_+ P_{i,i+1}^{T=0} - a_+ |b_+|) \quad (3) \end{aligned}$$

Completely ferromagnetic (FM) S spins and disordered T spins given by the T -spin 1/2 antiferromagnetic (AF) Bethe ansatz solution make the expectation values of the second and third terms minimum at the same time. For these wave functions the first term is automatically minimized. Therefore the ground states are constructed by such configurations as the S and T spin parts are given by FM-ordered state with $S_{tot} = N/2$ and the spin 1/2 AF-disordered liquid state with $T_{tot} = 0$. In fact, Fig.1 shows that these wave functions remain to be the ground states in a little wider region (still $a \geq -1$ but $b \geq -1$).

The asymptotic behavior of the I-IV phase boundary far away from origin is estimated through the consideration of the instability of the phase IV when approaching this boundary from the exactly solvable region. To this end, we consider the infinitely large a and finite b limits and apply the perturbative approach. The ground-state wave function for the non-perturbative term, including a , becomes the AF Bethe ansatz one about the T spin. Then the perturbative term, not including a ,

have the form, $\sum_i (b/4 - \epsilon_g) \vec{S}_i \vec{S}_{i+1}$, where $-\epsilon_g$ is the ground-state energy per site for AF Heisenberg model, defined by $\langle \vec{T}_i \vec{T}_{i+1} \rangle_{g.s.}$. Therefore, in the region with $b < 4\epsilon_g$ and large a , the ground-state wave function can be the same in the phase IV. We have checked that the I-IV phase boundary converges to $b = 4\epsilon_g$ for the finite 8- and 12-site systems. Since we know the exact value of $\epsilon_g = \log 2 - 1/4$ in the bulk limit, we conclude that $b = 4\epsilon_g = 1.7726$ is the asymptote of this phase boundary. It is important to note that for the region $b > 4\epsilon_g$, the initial wave functions with the decoupled S and T spin ones are no more valid and such perturbative approach does not always work. According to the symmetry of $H(a, b)$, in the phase II the model shows the same properties as in the phase IV with changing the S and T spins.

At $(a, b) = (3, 3)$, we can rewrite $H(a, b)$ as

$$H(a, b) = \sum_i P_{i,i+1}^{S=1} P_{i,i+1}^{T=1}, \quad (4)$$

where $P_{i,i+1}^{S=1}$ ($P_{i,i+1}^{T=1}$) represents the projection operator onto the S (T) spin triplet subspace for the neighboring sites. The configuration where either S or T spins are singlet at every bond makes the energy minimum to be zero. Thus we find that the nested dimer singlet states, where S and T spin parts are dimerized so as not to overlap their singlet bonds, are the exact ground states.⁷⁾ These states are obviously twofold degenerate and the relative difference of the momentum equals to π . Since the LSM theorem⁹⁾ is applicable to the present model for arbitrary a and b , there exists a finite gap above these degenerate ground states. Lastly, in the infinitely large a and b limit, Eq.(1) was studied as the two-leg spin ladder model with 4-body interaction and found to have a finite gap.¹⁰⁾

§3. Excitations and new gapless phases

3.1 Excitations in the phase II, III, and IV

Next we investigate properties of the excitations in the $a - b$ plane. For this purpose, we classify the excitations according to their quantum numbers (S_{tot}, T_{tot}) . The several lowest-lying energies of $H(a, b)$ are calculated by using the Lanczos method in all the subspaces with changing (S_{tot}^z, T_{tot}^z) . Note that there are $N/2 \times N/2$ number of subspaces for the N -site system. Through these calculations we can specify the quantum number (S_{tot}, T_{tot}) of the excited state at a point (a, b) . We have performed above calculations in the square region, $-4 \leq a, b \leq 4$, with varying a and b by the mesh of 0.1. As a result, we obtain the 80×80 meshes, on each mesh the quantum number (S_{tot}, T_{tot}) of the lowest-lying excited state is specified. The obtained boundaries of the excitations for the 8-site system are shown in Fig.2. In the figure, we label the states so as to be invariant for the general system size N . The spin or orbital excitations with seemingly strange quantum numbers (2,0) or (0,2), respectively, are intrinsic independently of N .

In the phase III, the usual FM-magnon excitations

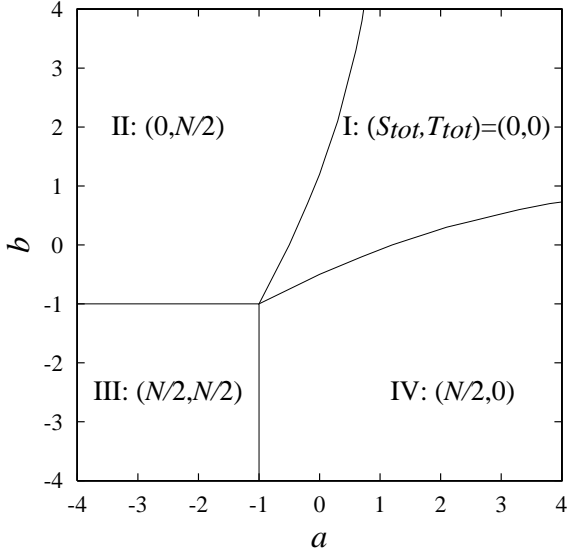


Fig. 1. Ground-state phase diagram of $H(a,b)$ with the PBC. Each phase is classified according to the quantum number (S_{tot}, T_{tot}) as shown in the figure.

of either S or T spin degrees of freedom are observed depending on $a < b$ or $a > b$, respectively. These excitations are exactly consistent with those expected from the completely FM ground state. In the phase IV, both FM S -spin magnon excitations and AF T -pseudo-spin magnon excitations appear next to each other. This boundary can be understood in the following manner. First of all, we note that the AF magnons have a momentum(q)-linear dispersion while the FM magnons have a q -square dispersion. Therefore the FM-magnon excitation always gives lower energy than the AF magnon for a sufficiently small momentum. Unless the system size is large enough and the minimum discrete momentum is not smaller than the crossing point of the FM- and the AF-magnon dispersion, the first excited state is the AF magnon. In the bulk limit, however, the FM magnon necessarily gives the minimum excitation. In fact, the numerically calculated region of the AF T -pseudo-spin magnon excitations are suppressed with increasing the system size. Therefore we conclude that the lowest excitation in the phase IV is the FM S -spin magnon in the bulk limit. By exchanging S and T spins in the region IV, we know the excitation properties in the phase II.

The boundary between $(2,0)$ and $(N/2-1,0)$ in Fig.2 is compatible with the phase boundary between I and IV of the ground-state phase diagram (Fig.1). On this boundary, there is the narrow region where the lowest excitation has either $(S_{tot}, T_{tot}) = (0,0)$ or $(N/2,0)$, which are the quantum numbers of the neighboring ground states. This is because magnetic and non-magnetic ground state cross on it and the energies of the ground states on the other side phase become lower than those of the magnon excitations owing to the finite size effects. From the arguments until now, the ground state and excitations in the phases II, III, and IV, are clearly understood. It should

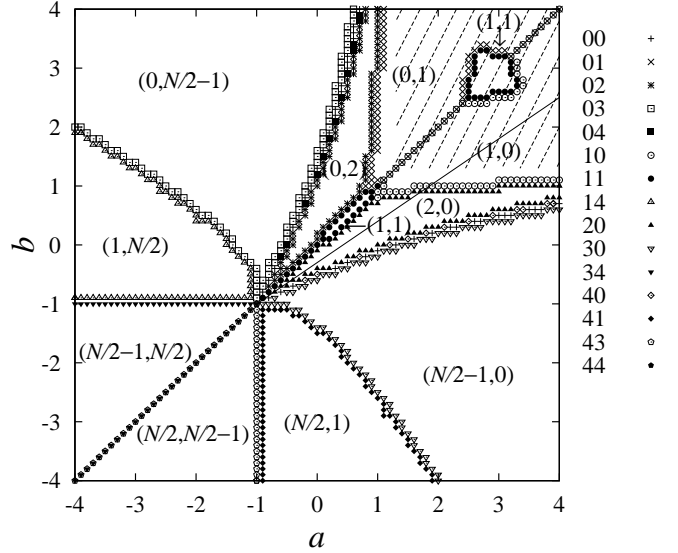


Fig. 2. The excited-state phase diagram for the system size $N = 8$ with the PBC. The right-hand side symbols stand for the quantum number (S_{tot}, T_{tot}) . The region $(2,0)$ continues to about $(a,b) = (7.2, 1.2)$ with decreasing its width. In the shaded region, the ground states are nearly twofold degenerate.

be noted that above simple pictures come from the decoupled wave functions about spin and orbital degrees of freedom. The remaining problems are the properties in the phase I, especially nearly around the $SU(4)$ symmetric point where the decoupled spin-orbit picture is obviously wrong, which are the subjects in the rest of this paper.

3.2 Symmetric line in the phase I

It is naturally expected that the $SU(4)$ symmetric point becomes the multi-critical fixed point and how different phases emerge from it determine the character of each phase. We would like to emphasize that one of the main concerns hereafter is the fact whether a finite gap exists or not above the ground state in the thermodynamic limit. First, in order to consider the properties on $b = a$ line (symmetric line), which has relatively higher symmetry in the phase I. We keep track of the several lowest eigenstates with the specified quantum numbers (S_{tot}, T_{tot}) by using the exact diagonalization. The obtained excitation-energy diagrams for the 8- and 12-site system with the PBC are shown in Fig.3. At $a = 1$, we know that $H(a, a)$ has gapless excitations with $(S_{tot}, T_{tot}) = (1, 1)$, $(1, 0)$, $(2, 0)$, and others.¹⁾ Similarly the states with these quantum numbers are softened at $a = -1$. From Fig.3 the excitation energies (ΔE) seem to be uniformly suppressed in the interval of $-1 < a < 1$ as the system size is increased. Thus it is natural to consider that the symmetric line is critical in the range of $-1 \leq a \leq 1$. We have confirmed that the excitation energies corresponding to $(S_{tot}, T_{tot}) = (1, 1)$ and $(2, 0)$, $(= (0, 2))$, all goes to zero linearly by the DMRG calculations for the system size up to 20 sites at $a = -0.5, 0$,

0.5, and 1. The obtained excitation gap after the system size extrapolation are presented in Fig.3-(b), in which we fit the finite-size data with the polynomial function of $1/N$ by the least mean square method. In the DMRG calculations, we keep at least 400 number of states in each renormalization.

This gapless behavior is consistent with the numerical calculation by Pati *et al.* and the analytic approach by Azaria *et al.* On this line, we perform the momentum-specified Lanczos method using translational symmetry and specify the (1,1)- and (2,0)- excitation to have the momentum $\pi/2$ and π , respectively. From the LSM theorem, these excitations must not be the isolated states but form continua. As a matter of fact, there are three independent massless continua with the same velocity of sound at the SU(4) point.¹¹⁾ Both the lowest and highest of them, softening at $q = \pi/2$, belong to $[2^1 1^2]$ irreducible representation, consisting of $(S_{tot}, T_{tot}) = (0, 1) \oplus (1, 0) \oplus (1, 1)$. On the other hand, the middle one softening at π belongs to $[2^2] = (0, 0) \oplus (1, 1) \oplus (2, 0) \oplus (0, 2)$.¹⁾ Therefore, we conclude that, along the symmetric line, (1,1)- and (2,0)- (same for (0,2)-) excitations are split from the $[2^1 1^2]$ and $[2^2]$ irreducible representations at the SU(4) point, respectively.

For $a > 1$, the (0,0)-excitation with momentum π falls down just after the level crossing around $a = 1$. At the SU(4) point we know that this state belongs to $[2^2]$ irreducible representation and its excitation energy is of the order of the inverse of the system size. Therefore the crossing points of the lowest branches are expected to converge to the SU(4) point in the bulk limit. This is perhaps because that this point becomes the fixed point in the sense of the renormalization group. For the region $a > 1$, two lowest states with the same quantum number (0,0) become nearly degenerate as the increase of N shown in Fig.3. In particular, at $a = 3$ they completely degenerate even in the finite system sizes. Around there (1,1)-excitation becomes the lowest (see Fig.2), which may be the spin-orbit bound states.

From these evidences, it is reasonable to conclude that in the range of $a > 1$ on the symmetric line, the ground states are doubly degenerate breaking the translational symmetry. One of them corresponds to the ground state with $[1^4]$ irreducible representation and the other is the isolated state originating from $[2^2]$ at the SU(4) point. Since the LSM theorem is applicable all over the $a - b$ plane as mentioned earlier, the doubly degenerate ground states mean the existence of the finite excitation gap above them in the bulk limit, while the other case of the LSM theorem, the singlet ground state with continuous excitation spectrum, are realized for $a \leq 1$.

In order to study how the excitation gap opens along the symmetric line, the DMRG calculation for larger systems under the PBC is performed. We estimate the first excitation energy by the difference between the two lowest states in the subspace of $(S_{tot}^z, T_{tot}^z) = (0, 0)$ and (1,0), respectively. The excitation gaps for $a > 1$ calculated in the same way for $a \leq 1$ are shown in Fig.3-(b). In the re-

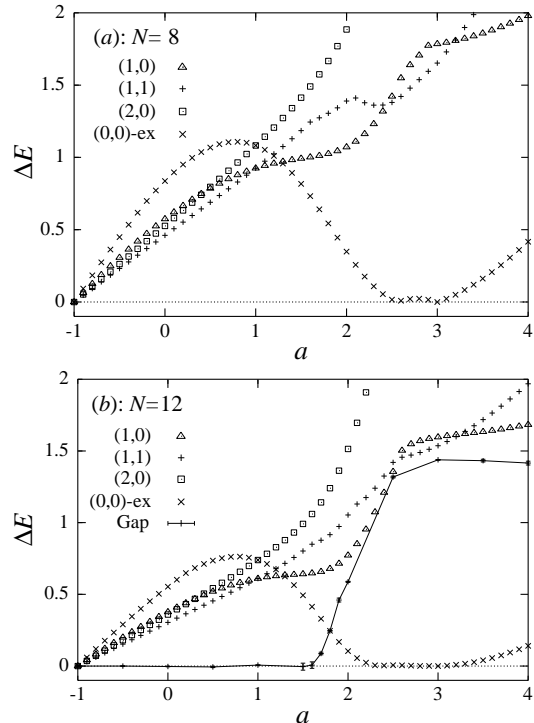


Fig. 3. The excitation-energy diagram with the specified quantum numbers (S_{tot}, T_{tot}) on the symmetric $b = a$ line. Figure (a) and (b) correspond to 8- and 12-site system, respectively. (0,0)-ex represents the excited state with $(S_{tot}, T_{tot}) = (0, 0)$. Figure (b) also includes the excitation gap after the system-size extrapolation.

gion of $a \geq 1.7$ there seems to exist a finite gap, but it is hard to conclude whether a finite gap exists or not in the region $1 \leq a \leq 1.6$ even by the DMRG calculations up to 20-site system. From these results we conclude that for $a > 1$ the excitation gap opens exponentially slowly, while for $a \leq 1$ no finite gap exists.

Let us consider a possible scenario by using the simple renormalization group concepts, in which we can explain the numerically obtained excitation properties along the symmetric line. Suppose that we introduce the perturbation along this line into the SU(4) symmetric point, $a = 1$. Then consider what kinds of the properties, such as relevant, irrelevant or marginal, the introduced perturbation should have so as to reproduce the numerical results. It is likely that the dominant perturbation operator becomes a marginally irrelevant in the (-1,-1) direction, while it becomes a marginally relevant in the opposite direction. This picture is consistent with the numerical results, that is, for $a \leq 1$ there does not exist a finite gap and for $a \geq 1$ a gap opens exponentially slowly. This scenario also agrees with the bosonization result by Azaria *et al.*

On the contrary, Pati *et al.* claimed that the excitation is gapless for $a \leq 1$, though for $a > 1$ the gap (ΔE) opens by a power-law function, $\Delta E \propto (a - 1)^{1.5}$. They assumed that the first excited state was in the subspace of $(S_{tot}^z, T_{tot}^z) = (1, 1)$. However, such assumption does not give correct lowest-excitation energy in almost all

the region I except for the $b = a$ line ($-1 \leq a \leq 1$) and the neighborhood of $(a, b) = (3, 3)$ (see Fig.2). Their conclusion is unlikely from the viewpoint of the simple perturbative discussion. The gapless behavior for $a < 1$ requires irrelevant or marginally irrelevant perturbative operators. Since the additional opposite-signed perturbation has the same scaling dimension, the excitations in the opposite (1,1)-direction can not be gapful with a power-low dependence.

Along the symmetric line, we have also calculated the correlation functions by the DMRG method under open boundary conditions up to 36 sites. For eliminating the boundary effects, we adopt the averaging procedure and obtain their Fourier transformations by arranging them in a ring. The peak structures exist at $q = \pi/2$ for $1 < a \leq 2.0$, though the peaks lose their sharpness and become broadened over $a > 1.6$. Note that, a large finite-size effect with the slow growth of the excitation gap make it difficult to determine the transition point ($a = 1$) by this approach, too. For the region $a > 2.1$, the peaks locate at $q = \pi$ and no other structures are found elsewhere. The incommensurate line from $a = 1$ to 2 discussed by Pati *et al.* is not found. Our numerical result again supports the analysis by Azaria *et al.*

3.3 Novel gapless phases in the asymmetric regions of the phase I

Beside the symmetric critical line, we discover the novel distinct phases characterized by the strange excitation-quantum numbers, $(S_{tot}, T_{tot}) = (2, 0)$ or $(0, 2)$, as shown in Fig.2. In order to investigate these phases, the excitation-energy diagrams are examined for 8- and 12-site system with PBC along the asymmetric $b = 0.7a - 0.3$ line, which is shown in Fig.2 by the solid line. The obtained diagrams, Fig.4-(a) and (b), are different from those on the symmetric line in that the level-crossing point is at about $a = 1.9$ and below it the (2,0)-excitation becomes the lowest. The lowest (2,0)-excitations with momentum π are continuously connected to those on the symmetric line and therefore form the continuous excitation spectra softening at $q = \pi$. The lowest excitation gap goes to zero linearly at $a = 0$ and 1 on $b = 0.7a - 0.3$ line by the DMRG calculation up to 20-site system. The other gapless excitation with $(S_{tot}, T_{tot}) = (1, 1)$ on the symmetric line also seems to have zero gap from the DMRG calculation up to system size with $N = 20$ at least $a = 1$. The finite excitation gaps are obviously established over $a > 3$, since even For $N = 8$ and 12 sites the excitation energies converge as the function of $1/N$ as shown in Fig.4-(a) and (b).

By using the DMRG method under the PBC, we research how the excitation gap opens along the asymmetric line from $a = -1$ to 4. The calculated conditions are the same for the symmetric line and the obtained results are shown in Fig.4-(b). We find that the excitation gap opens exponentially slowly just after the sudden decrease of the (0,0)-excitations to be one of the degenerate ground states in the bulk limit. We can easily understand

the behaviors of the excitation gap by looking at those of the (1,0)-excitations in Fig.3 and Fig.4. In short, all these gap-formative excitations show the exponentially slow growths after the level-crossing around $a = 1$ or 1.9. Accordingly, the newly found (2,0)- and (0,2)-phases are gapless and in crossing the gapless-gapful phase boundary in the phase I, the gap opens exponentially slowly as well as on the symmetric line.

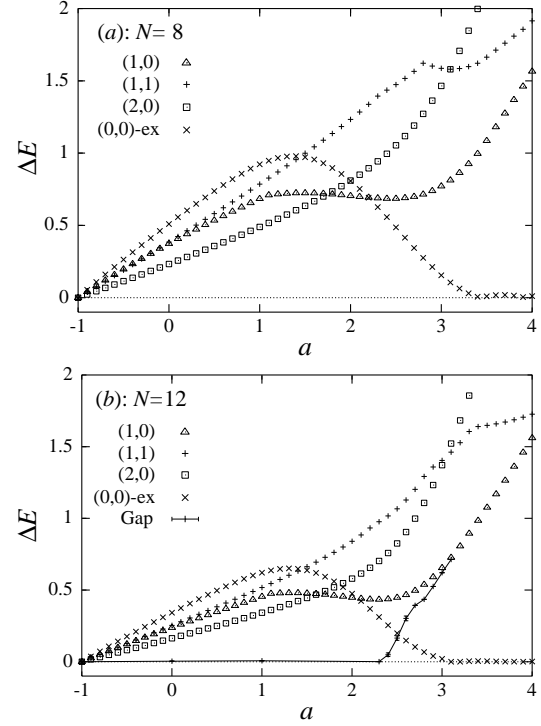


Fig. 4. The excitation-energy diagram on the asymmetric $b = 0.7a - 0.3$ line. The notations are the same as Fig.3.

We have confirmed by the Lanczos method for 12-site system that the more downward the boundary between (2,0)- and (1,0)-phases moves, the farther we are away from the $SU(4)$ point. By the DMRG calculation up to the system size $N = 20$, the lowest excitation energy at $(3,0.8)$ in the subspace of $(S_{tot}^z, T_{tot}^z) = (1, 0)$ is lower than that in (2,0). On the other hand, those at $(1,0.4)$ and $(2,0.6)$ are involved in (2,0)-phase and go to zero linearly as the function of $1/N$. Our numerical results suggest that the gapless-gapful phase boundary in the phase I starts from the $SU(4)$ point with some finite angle less than right angle against the symmetric line, having a positive curvature. It nearly converges to the ground-state phase boundary over $a \approx 3$. Although we cannot numerically determine its exact angle, the previously used simple picture based on the renormalization group tells us a reasonable scenario as follows. The key point is that it is presumably expected that when the perturbative operator in one direction are marginally irrelevant, that in the opposite direction will become marginally relevant. Since no other phases are found in both gapless and gapful phases numerically, it is natural to suppose that the

boundary starts from the SU(4) point perpendicularly to the symmetric line, so as not to contradict the symmetry about the exchange of the S and T spins. We think that our numerical results are naturally explained in accordance with this scenario.

It should also be mentioned here that other possibilities still remain at this stage, since it is too difficult to distinguish a true zero gap from a finite but exponentially small gap. The analytic approach around the fixed point including the asymmetric regions just meets this demand. Such analytic approach by using the bosonization method is now being developed by Y. Tsukamoto and N. Kawakami.¹²⁾ Their result seems to be consistent with ours about the properties of each phase. It also consistently suggests the gapless-gapful boundaries begin exactly in the vertical direction to the symmetric line just around the SU(4) fixed point.

From the discussions above, we conclude that the intrinsic phase diagram of the SU(2)⊗SU(2) model is given by Fig.5. Although there still remain some ambiguities about the I₀-I_S and I₀-I_T phase boundaries.

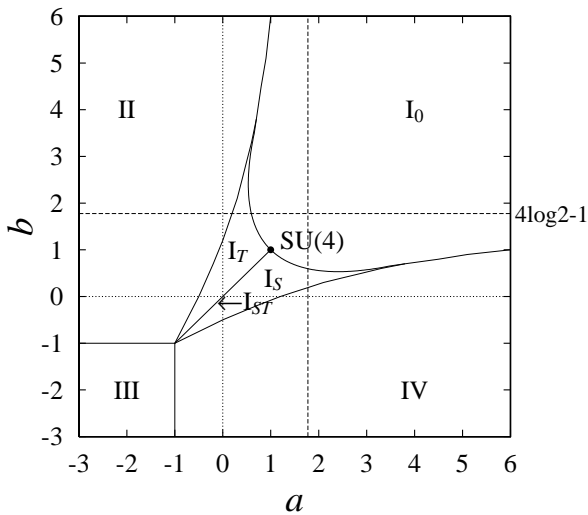


Fig. 5. The phase diagram of SU(2)⊗SU(2) coupled spin-orbit model given by Eq.(1) in the bulk limit. The region I in Fig.1 is decomposed into four phases, I₀, I_S, I_T, and I_{ST}. The broken lines represent the asymptotes of the I-IV and I-II boundary

§4. Summary

In summary, we have studied the one-dimensional SU(2)⊗SU(2) symmetric spin-orbit coupled model by means of the numerical calculations using the Lanczos and the DMRG methods. In the phase II, III, and IV, we have made clear the ground-state and excitation properties by noticing the fact that the ground-state wave functions are depicted by the decomposed S and T spins. In addition we also determine the asymptote of phase I-IV boundary through the discussion about the instability of the phase IV. On the symmetric line in the phase I, there exists a finite excitation gap for $a > 1$, which

grows exponentially slowly above the doubly degenerate ground states in consistent with the LSM theorem. On the other hand for $a < 1$, the other case of the LSM theorem are realized with the continuous spin, orbit, and coupled spin-orbit excitations corresponding to the excitation-quantum numbers, $(S_{tot}, T_{tot}) = (2, 0), (0, 2),$ and $(1, 1)$, respectively. We find that the estimated gap growth disagrees with that by Pati *et al.* and reproduce the result by Azaria *et al.*

We extend our analysis in the asymmetric regions and find that the phase I is composed of the four distinct phases centering the SU(4) symmetric point (see Fig.5). Three massless phases, I_S, I_T, and I_{ST}, are characterized by the gapless continua, above a singlet ground state, with the quantum number, $(S_{tot}, T_{tot}) = (2, 0), (0, 2),$ and $(1, 1)$, respectively. Considering the continuous branches with the highly degenerate irreducible representations at the SU(4) point, we conclude that the pure spin or orbital excitations originate from the same branch softening at $q = \pi$ with the $[2^2]$ irreducible representation, while the coupled spin-orbit excitation from the other one softening at $q = \pi/2$ with $[2^1 1^2]$. In the rest part of I, labelled as I₀, the finite excitation gap opens above the doubly degenerate ground states by breaking translational symmetry. These gapless and gapful situations exactly correspond to the alternative of the LSM theorem. We also estimate how the excitation gap opens in crossing the gapless-gapful boundary in the phase I to find that the gap opens exponentially slowly in the same way on the symmetric line.

Acknowledgements

The authors wish to acknowledge Norio Kawakami and Yasumasa Tsukamoto for many valuable discussions. This work is financially supported by a Grant-in-Aid for Scientific Research from the Ministry of Education, Science, Sports and Culture in Japan.

-
- [1] Y. Yamashita, N. Shibata, and K. Ueda, Phys. Rev. B **58**, 9114 (1998)
 - [2] Y. Q. Li, Michael Ma, D. N. Shi, and F. C. Zhang, Phys. Rev. Lett. **81** 3527 (1998)
 - [3] B. Frischmuth, F. Mila, and M. Troyer, Phys. Rev. Lett. **82**, 835, (1999).
 - [4] Y. Yamashita, N. Shibata, and K. Ueda, LANL cond-mat/9905211.
 - [5] S. Pati, R. Singh, and D. I. Khomskii, Phys. Rev. Lett **81**, 5406 (1998)
 - [6] P. Azaria, A. Gogolin, P. Lecheminant, and A. Nersisyan, LANL cond-mat/9903047.
 - [7] A. K. Kolezhuk and H.-J. Mikeska, Phys. Rev. Lett. **80**, 2709 (1998).
 - [8] S. R. White, Phys. Rev. Lett. **69**, 2863 (1992), and S. R
 - [9] E. H. Lieb, T. Schultz, and D. J. Mattis, Ann. Phys. (N.Y.) **16**, 407 (1961).
 - [10] A. A. Nersisyan and A. M. Tsvelik, Phys. Rev. Lett. **78**, 3939 (1997).
 - [11] B. Sutherland, Phys. Rev. B **12**, 3795 (1975).
 - [12] Private communication with Y. Tsukamoto and N. Kawakami